

Original Paper

---

# Necroptosis of Lung Epithelial Cells Triggered by Ricin Toxin and Bystander Inflammation

Cody G. Kempen<sup>a</sup> Matthew A. Deragon<sup>a</sup> Alexa L. Hodges<sup>a</sup> Michael Hamersky<sup>a</sup>  
Melanie Vugelman<sup>a</sup> Jack Qu<sup>a</sup> Nicholas J. Mantis<sup>b</sup> Timothy J. LaRocca<sup>a</sup>

<sup>a</sup>Albany College of Pharmacy and Health Sciences, Albany, NY, USA, <sup>b</sup>Wadsworth Center, Albany, NY, USA

## Key Words

Ricin toxin • Toxins • Cytokines • Toxin-mediated diseases • Apoptosis • Necroptosis • Tumor necrosis factor • Fas • Fas ligand • Caspases • HMGB1 • Bystander cell death

## Abstract

**Background/Aims:** The ribosome-inactivating proteins include the biothreat agent, ricin toxin (RT). When inhaled, RT causes near complete destruction of the lung epithelium coincident with a proinflammatory response that includes TNF family cytokines, which are death-inducing ligands. We previously demonstrated that the combination of RT and TNF-related apoptosis inducing ligand (TRAIL) induces caspase-dependent apoptosis, while RT and TNF- $\alpha$  or RT and Fas ligand (FasL) induces cathepsin-dependent cell death in lung epithelial cells. We hypothesize that airway macrophages constitute a major source of cytokines that drive lung epithelial cell death. **Methods:** Here, we show that RT-induced apoptosis of the monocytic cell line, U937, leads to the bystander killing of the lung epithelial cell line, A549. U937 cells were treated with ricin. Following this, A549 cells were treated with supernatants from U937 cells and death was measured by WST-1 viability assay **Results:** Upon RT-induced U937 cell death, released RT and FasL contributed to A549 cell death. U937 cells also released nuclear protein HMGB1. The release of RT, FasL, and HMGB1 triggered A549 cell necroptosis, rather than cathepsin-dependent killing observed previously with RT and FasL. Reactive oxygen species (ROS) were produced in A549 cells due to HMGB1 ligation of the receptor for advanced glycation end products (RAGE). **Conclusion:** These findings demonstrate the potential for bystander necroptosis of lung epithelial cells during RT toxicosis which may perpetuate or increase the proinflammatory response.

© 2023 The Author(s). Published by  
Cell Physiol Biochem Press GmbH&Co. KG

## Introduction

Ricin toxin (RT) comprises 1-5 % of the total dry weight of the castor bean plant, *Ricinus communis* [1–3]. In its mature form, RT is a 60-65 kDa glycoprotein capable of inhibiting protein synthesis in mammalian cells (1-3). RT is classified by the Centers for Disease Control and Prevention (CDC) on the list of select agents and toxins due to its extreme toxicity when inhaled as an aerosol [1–5].

RT is the prototypic A-B toxin, comprised of a catalytic A subunit (RTA) linked via a single disulfide bond to the cell-binding B subunit (RTB) [6, 7]. RTB binds  $\beta$ 1-4 galactose and N-acetylglucosamine that are part of glycolipids and glycoproteins on the cell surface [8]. RT enters the cell via the endocytic pathway and is thus trafficked to the Golgi as well as the endoplasmic reticulum (ER) [9]. In the ER, the disulfide bond between RTA and RTB is reduced by protein disulfide isomerase and the two subunits dissociate [9, 10]. RTA is then translocated across the ER membrane and delivered into the cytoplasm where it inactivates ribosomes with high efficiency [10, 11]. Specifically, RTA cleaves a glycosidic bond in the sarcin-ricin loop (SRL) resulting in the removal of an adenine from 28s rRNA [10, 11]. This damage to the ribosome prevents the binding of elongation factor 2 causing protein synthesis to cease [11–13]. RT is highly toxic when inhaled [14–16]. The damage to the airway by RT leads to acute respiratory distress syndrome (ARDS) and a potent inflammatory response [16–19].

As stated, RT causes a vast amount of damage to lung epithelial cells when inhaled [16–19]. Additionally, our previous work showed that the cytokines TNF-related apoptosis-inducing ligand (TRAIL), TNF- $\alpha$ , and Fas ligand (FasL) modulate the toxicity of RT [20, 21]. We demonstrated that addition of TRAIL sensitized A549 and Calu-3 human lung epithelial cells to RT-induced caspase-dependent apoptosis [21]. However, RT combined with TNF- $\alpha$  or FasL induced a cathepsin-dependent, caspase-independent death that was inhibited by the pan-caspase inhibitor, zVAD-fmk [21]. We propose that cytokines contribute to the vast damage of ARDS *in vivo*, considering that proinflammatory and death-inducing cytokines are abundant components in the bronchoalveolar lavage fluid of animals following inhalation of RT [15, 22–26]. Monocytes and macrophages are other key target cells for RT [22, 27]. In fact, macrophages are responsible for the high level of inflammatory cytokines during RT toxicity [28]. Thus, we hypothesize that RT-induced death of monocytes/macrophages contributes to bystander damage to lung epithelial cells. Here, we use biochemical approaches to provide a detailed characterization of U937 and A549 cell death responses to RT. U937 cells were chosen for this study as they are a model for human monocytic cells and have been used successfully in the characterization of eukaryotic programmed cell death [29–35]. We show that RT-induced apoptosis of U937 cells leads to RT-induced necroptosis of bystander A549 cells due to the release of several factors. Defining these cell death responses and identifying multiple steps at which they can be prevented may lead to new therapeutic approaches to RT toxicity.

## Materials and Methods

### *Reagents, antibodies, and inhibitors*

Ricin toxin (*Ricinus communis* agglutinin II) was purchased from Vector Laboratories and used at the concentrations noted. RT was dialyzed in 1x PBS using 10K MW-cutoff Slide-A-Lyzer dialysis cassettes (Pierce, Rockford, IL, USA) prior to experimentation. Recombinant human FasL (Super Fas ligand, Enzo Life Sciences, Farmingdale, NY, USA) was used at a concentration of 100 ng/mL unless noted otherwise. Recombinant human HMGB1 (Millipore-Sigma) was used at a concentration of 100 ng/mL.

All inhibitors were purchased from ApexBio (Houston, TX, USA) unless otherwise noted. Pan-caspase inhibitor zVAD-fmk, was used at a concentration of 50  $\mu$ M. Caspase-3/7 inhibitor zDEVD was used at a concentration of 30  $\mu$ M. Caspase-1 inhibitor, zYVAD-fmk was used at a concentration of 10  $\mu$ M. The ferroptosis inhibitor, ferrostatin-1, was used at a concentration of 1  $\mu$ M. Cathepsin inhibitor 1 (CATI-1)

was used at a concentration of 20  $\mu$ M. N-acetylcysteine (Millipore-Sigma) was used at a concentration of 10 mM. NADPH oxidase inhibitor, VAS2870 (Millipore-Sigma), was used at a concentration of 5  $\mu$ M. The RIP1 inhibitor, necrostatin-1s (Millipore-Sigma), was used at a concentration of 50  $\mu$ M. The RIP3 inhibitor, GSK'872 (MedChemExpress), and the MLKL inhibitor, GW806742x (MedChemExpress), were each used at a concentration of 1  $\mu$ M.

All neutralizing mAbs were used at a concentration of 1  $\mu$ g/mL. FasL neutralizing mAb, NOK-1, was purchased from Becton-Dickenson while TNF- $\alpha$  neutralizing mAb, J1D9, and TRAIL neutralizing mAb, HS501 (Cat # ALX-804-300-C100) were purchased from Axxora (Farmingdale, NY, USA). RTA and RTB neutralizing mAbs were kindly provided by the Wadsworth Center (NYS Department of Health). The RAGE mAb was purchased from R and D Systems (Minneapolis, MN, USA, Cat # AF1145) while the HMGB1 mAb was purchased from AbCam (Cambridge, UK, Cat # ab18256).

### *Cell culture*

A549 lung epithelial cells (ATCC, Manassas, VA, USA) were cultured in Ham's F-12K medium (Sigma) with 10 % FBS. Cells were grown in a humidified incubator with 5 % CO<sub>2</sub> at 37 °C. Cells were cultured in 75-cm<sup>2</sup> cell culture flasks and subcultured when they reached ~80 % confluence at a 1:5 dilution. Cells were lifted using TrypLE Express (Thermo Fisher, Waltham, MA, USA) at 37 °C. U937 suspension cells (ATCC) were cultured in RPMI 1640 medium supplemented with 10% fetal bovine serum in a humidified incubator at 37 °C and 5 % CO<sub>2</sub>. Cells were maintained at a maximum of 10 passages for the experiments in this work. Cells were cultured in 75-cm<sup>2</sup> cell culture flasks and subcultured when they reached 1 x 10<sup>6</sup> cells/mL at a 1:5 dilution.

### *Cell death assays*

A549 lung epithelial cells were seeded at 1200 cells/well in 96-well plates (Celltreat, Pepperell, MA, USA) and allowed to culture for 24 h in Ham's F-12K medium (Thermo Fisher) with 10 % FBS (VWR, Radnor, PA, USA) at 37 °C and 5 % CO<sub>2</sub>. Following this, cells were washed and the following was added to wells in Ham's F-12K medium: (1) RT or (2) RT combined with 100 ng/mL FasL. Cells were incubated at 37 °C with 5 % CO<sub>2</sub> for 24 h followed by WST-1 assay (Takara, Kusatsu, Shiga Prefecture, Japan) according to the manufacturer's instructions.

U937 cells at a concentration of 5x10<sup>5</sup>/mL were treated with RT in 96-well plates (Celltreat). Following treatment, cells were incubated for 24 h at 37 °C with 5 % CO<sub>2</sub>. This was followed by WST-1 assay (Takara) according to the manufacturer's instructions.

For bystander cell death assays, U937 cells (5x10<sup>5</sup>/mL) were treated with RT for 1 h at 37 °C with 5 % CO<sub>2</sub> in RPMI 1640. Following this, free RT was removed by centrifugation and washing. U937 cells were then allowed to incubate an additional 4 h at 37 °C with 5 % CO<sub>2</sub> in Ham's F-12K medium. Cells were centrifuged and the supernatant was removed. A549 lung epithelial cells (seeded at 1200 cells/well) were then treated with 100  $\mu$ L of supernatants from U937 cells treated with RT. A549 cells were incubated with the supernatants for 24 h at 37 °C with 5 % CO<sub>2</sub>. This was followed by WST-1 assay (Takara) according to the manufacturer's instructions.

For all cell death assays, cells in negative control wells were treated with media alone. In experiments where inhibitors or mAbs were used, they were added to cells 1 h before the addition of RT and FasL or supernatants from U937 cells treated with RT. DMSO was used as vehicle control for each inhibitor. For all cell death assays absorbance was measured using an Eppendorf 2200 plate reader at a wavelength of 450 nm and a reference wavelength of 600 nm. Using WST-1 absorbance (abs), percent viability was calculated as follows: (abs cell death stimulus)/(abs neg) x 100.

### *Flow cytometry*

For flow cytometry analyses 10,000 events were collected for each sample after gating out debris. Sample data were collected utilizing a BD FACSVerse flow cytometer. Data files were analyzed using FlowJo V10. Prior to analysis, cells were treated with: (1) RT, (2) RT + FasL, or (3) supernatants derived from U937 cells treated with RT at 37 °C and 5 % CO<sub>2</sub> for 6 h. For caspase activity, the Vybrant FAM FLICA kit (Molecular Probes) was used according to the manufacturer's instructions. For Annexin/PI, the eBiosciences Annexin V apoptosis kit (ThermoFisher) was used according to the manufacturer's instructions. To measure oxidative stress, CellROX green kit (ThermoFisher) was used according to the manufacturer's instructions.

To measure mitochondrial ROS, MitoSOX superoxide indicator (ThermoFisher) was used according to the manufacturer's instructions.

### *SDS-PAGE and western blot*

A total of  $6 \times 10^6$  A549 cells were seeded in 58 cm<sup>2</sup> Petri dishes (Celltreat) and allowed to grow for 24 h at 37 °C and 5 % CO<sub>2</sub>. A549 cells were then treated with (1) 0.5 ng/mL RT, (2) 0.5 ng/mL RT combined with 100 ng/mL FasL or (3) supernatants derived from U937 cells treated with RT for 4 h at 37 °C and 5 % CO<sub>2</sub>. Following this, A549 cells were lysed using 1 % triton-X-100 (Sigma) with 1x Halt protease inhibitor (Thermo Fisher) in 1x PBS on ice for 30 min. Cells were then sonicated on ice 3x (20 sec pulses) at an output of 10 %. Cell lysates were centrifuged at 14000 rpm at 4 °C to remove nuclear material. A549 cell lysates were run on SDS-PAGE and transferred to a PVDF membrane and blocked in 1x TBS with 0.1 % tween-20 and 5 % milk for 30 min at room temperature. The blots were then incubated with diluted primary antibody in 1x TBS with 0.1 % tween-20 and 5 % milk overnight at 4 °C. All primary antibodies were obtained from Cell Signaling Technology (Danvers, MA, USA). Primary antibodies were used at dilutions of 1:1000 except for anti-GAPDH which was diluted 1:10000. After washing with 1x TBS with 0.1 % tween-20 and 5 % milk, the blots were incubated with secondary HRP-conjugate antibodies (1:5000) for 1 h at room temperature. Blots were developed by chemiluminescence and read in a Bio-Rad ChemiDoc XRS+.

### *ELISA*

For ELISA detection of HMGB1 and FasL in U937 cell supernatants, we used the HMGB1 Express ELISA kit (Tecan, Männedorf, Switzerland) and Fas ligand ELISA kit (AbCam) according to the manufacturers' instructions.

### *Statistical Analyses*

Statistical analyses were carried out using GraphPad Prism 7. All cell death assays, flow cytometry, and ELISA were subject to statistical analysis by two-way ANOVA and Bonferroni posttest. All cell death assays are the results of 3 independent experiments. Immunoblots presented are representative of 3 independent experiments.

## **Results**

### *RT-induced apoptosis of U937 cells leads to death of bystander A549 cells*

We first set out to characterize RT-induced death of U937 cells. These cells were treated with multiple concentrations of RT for 24 h at 37°C and assessed for viability using WST-1. Across a range of toxin concentrations, RT-induced death of U937 cells was prevented by the pan-caspase inhibitor, zVAD-fmk [36, 37], as well as the caspase-3/7 inhibitor, zDEVD-fmk [36, 37] (*Fig. 1A-B*). The RIP1 inhibitor, necrostatin-1s (nec-1s), which prevents necroptosis [38], had no effect on RT-induced death of U937 cells (*Fig. 1A*). To determine the activity of caspases, we treated U937 cells with RT (1 ng/mL) for 2 h at 37 °C followed by staining with FLICA reagent (specific for caspase-3/7 activity) and flow cytometry. There was a ~6-fold increase in fluorescence in RT-treated U937 cells (*Fig. 1C*). This indicates that caspases-3 and -7 are active [39]. This fluorescence was reduced by zVAD-fmk and zDEVD-fmk (*Fig. 1C*). To determine if phosphatidylserine is externalized upon RT treatment, U937 cells were treated with 1 ng/mL RT for 2 h at 37 °C followed by staining with annexin V and propidium iodide (PI) and flow cytometry. Upon RT treatment there is a greater than 10-fold increase in annexin staining, indicating the externalization of phosphatidylserine (*Fig. 1D*) [40]. Annexin staining was prevented when zVAD-fmk was administered indicating that phosphatidylserine externalization is caspase dependent (*Fig. 1D*). Propidium iodide staining, which assesses membrane permeability [41], was not significantly affected in any condition (*Fig. 1D*).

To test the hypothesis that RT-induced death of monocytes/macrophages leads to the death of bystander lung epithelial cells, we co-cultured U937 and A549 cells, treated them with different concentrations of RT for 24 h at 37 °C, and performed WST-1 viability assay. For this experiment, U937 cells were removed from co-culture and viability of the A549 cells only was assessed. Compared to A549 cells cultured alone, those co-cultured with U937 cells underwent a significant increase in cell death (*Fig. 2A*). To determine if the increase

in A549 death required cell-to-cell contact, we treated U937 cells with 1, 2, or 5 ng/mL RT for 1 h at 37 °C. After this, free RT was removed via centrifugation and washing and the cells were incubated an additional 4 h followed by removal of supernatants. A549 cells were then treated with the supernatants for 24 h at 37 °C followed by WST-1 viability assay. Supernatants from the U937 cells were toxic to A549 cells (Fig. 2B). In fact, supernatants from U937 cells treated with higher doses of RT (5 vs. 1 ng/mL, for example) induced higher levels of bystander A549 cell death (Fig. 2B). If U937 cells were treated with zVAD-fmk or zDEVD-fmk with RT, their supernatants were much less toxic to bystander A549 cells (Fig. 2C).

**Fig. 1.** RT causes caspase-3/7-dependent apoptosis in U937 cells. U937 cells were treated with different concentrations of RT for 24 h at 37°C followed by WST-1 assay. RT-induced death of U937 cells is prevented by A.) the pan-caspase inhibitor, zVAD-fmk, and B.) the caspase-3 inhibitor, zDEVD-fmk. The necroptosis inhibitor, necrostatin-1s (nec-1s) had no effect on cell death. U937 cells were treated with 1 ng/mL RT for 2 h at 37°C followed by C.) FLICA staining for caspase-3/7 activity or D.) staining for annexin V and propidium iodide (PI) and flow cytometry analysis. Caspase-3/7 activity increases following RT treatment but is prevented by zVAD-fmk and zDEVD-fmk (C). Annexin staining increases upon treatment with RT and is prevented by zVAD-fmk. There is no significant change in PI staining. Veh = vehicle control (DMSO). Results are from 3 independent experiments. Each dot in the graphs represents an independent experiment. Two-way ANOVA with Bonferroni posttest. \*\*\*p<0.001.

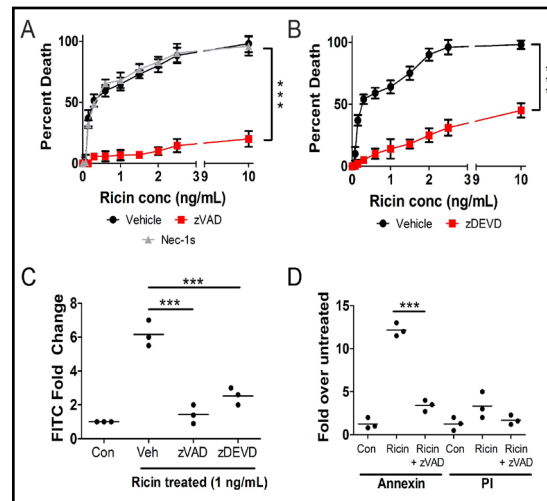
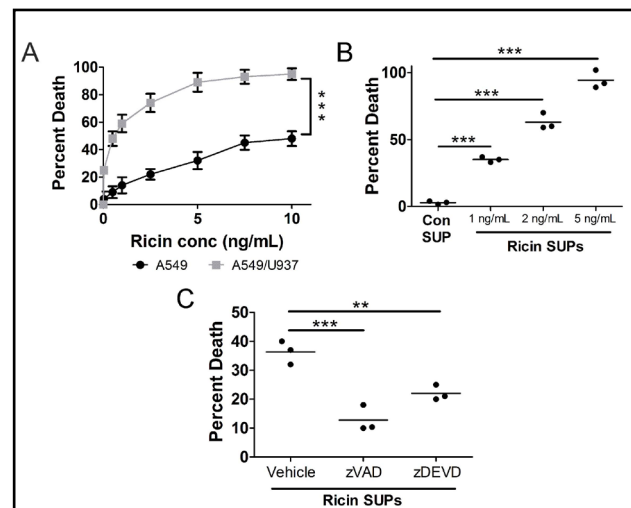


**Fig. 2.** RT-induced apoptosis of U937 cells leads to death of bystander A549 lung epithelial cells. A.) A549 cells were treated with different concentrations of RT alone or in co-culture with U937 cells for 24 h at 37°C. There is a significant increase in RT-induced A549 cell death when co-cultured with U937 cells. B.) U937 cells were treated with 1, 2, or 5 ng/mL RT for 5 h at 37°C. A549 cells were then incubated with U937 cell supernatants (RT SUPs) for 24 h at 37°C. Supernatants from RT-treated U937 cells induce death of A549 cells compared to supernatants from untreated U937 cells (con SUP). C.) U937 cells were treated with 1 ng/mL RT for 5 h at 37°C in the presence or absence of pan-caspase inhibitor, zVAD-fmk, and caspase-3 inhibitor, zDEVD-fmk. A549 cells were then incubated with U937 cell supernatants for 24 h at 37°C. A549 cell death induced by these supernatants was prevented if U937 cell death was blocked with zVAD or zDEVD. Vehicle = DMSO. Results are from 3 independent experiments. Each dot in the graphs represents an independent experiment. Two-way ANOVA with Bonferroni posttest. \*\*\*p<0.001, \*\*p<0.01.



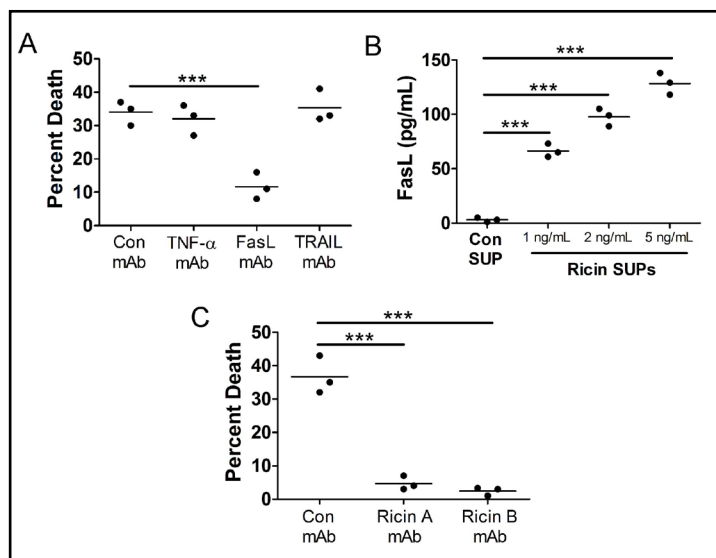
*Death of bystander A549 cells is due to the release of Fas ligand (FasL) and RT from U937 cells*

To determine the cause of toxicity in these supernatants, we treated U937 cells with 1, 2, or 5 ng/mL RT for 1 h at 37 °C. After this, free RT was removed via centrifugation and washing and the cells were incubated an additional 4 h. Cytokine neutralizing mAbs were added to these supernatants after which supernatants were used to treat A549 cells for 24 h at 37 °C followed by WST-1 assay. Supernatants derived from RT-treated U937 cells were less toxic to A549 cells following incubation with a neutralizing mAb against FasL (Fig. 3A). Neutralizing mAbs against TRAIL or TNF- $\alpha$  had no effect on the toxicity of the supernatants (Fig. 3A). This suggests that U937 cells attacked by RT release FasL which contributes to the death of bystander A549 cells. To measure the amount of FasL released from RT-treated U937 cells we performed a FasL ELISA. Supernatants derived from RT-treated U937 cells contained measurable amounts of FasL compared to supernatants from untreated U937 cells (Fig. 3B). Supernatants from U937 cells treated with higher doses of RT (5 vs. 1 ng/mL, for example) contained higher concentrations of FasL (Fig. 3B). To determine if RT released from U937 cells attacked by the toxin contributes to death of bystander A549 cells, we treated U937 cells with 1 ng/mL RT for 1 h at 37 °C. After this, free RT was removed via centrifugation and washing and the cells were incubated an additional 4 h. RT neutralizing mAbs were added to these supernatants after which supernatants were used to treat A549 cells for 24 h at 37 °C followed by WST-1 assay. Supernatants derived from U937 cells treated with RT and incubated with neutralizing mAbs to RTA and RTB exhibited a significant decrease in toxicity against A549 cells (Fig. 3C). This suggests that RT is released from dying U937 cells and contributes to the death of bystander A549 cells.

*Bystander A549 cell death differs from A549 cell death induced by purified FasL and RT*

The results of Fig. 3 suggest that U937 cells attacked by RT release FasL and RT into their supernatants which drives the death of bystander A549 cells. Previously, we showed that purified RT combined with FasL induces cathepsin-dependent death of A549 cells [21]. Therefore, we decided to compare A549 cell death induced by purified RT and FasL vs. A549

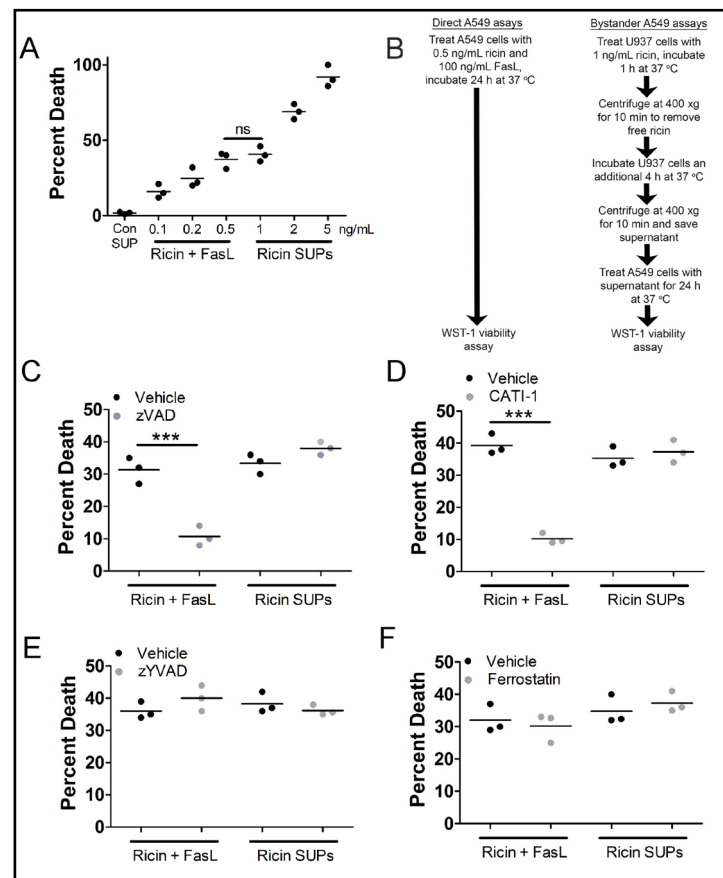
**Fig. 3.** Death of bystander A549 cells is driven by release of Fas ligand (FasL) and RT from RT-treated U937 cells. A.) U937 cells were treated with 1 ng/mL RT for 5 h at 37°C. A549 cells were then treated with U937 cell supernatants for 24 h at 37°C in the presence or absence of cytokine neutralizing mAbs (1  $\mu$ g/mL). Death of bystander A549 cells was prevented when FasL was neutralized in U937 cell supernatants. B.) U937 cells were treated with 1, 2, or 5 ng/mL RT for 5 h at 37°C. Supernatants were removed and subjected to FasL ELISA. There is a dose dependent increase in the release of FasL from



U937 cells following RT treatment. Con SUP = untreated U937 cells. C.) Cells were treated as described in part A except different neutralizing mAbs were used. Death of bystander A549 cells was prevented when RT was neutralized in U937 cell supernatants. RT A mAb = against catalytic domain, RT B mAb = against binding domain. Results are from 3 independent experiments. Each dot in the graphs represents an independent experiment. Two-way ANOVA with Bonferroni posttest. \*\*\*p<0.001.

cell death induced by supernatants derived from RT-treated U937 cells. For this, we treated A549 cells with 0.1, 0.2, or 0.5 ng/mL purified RT combined with 100 ng/mL purified FasL for 24 h at 37 °C which resulted in a dose-dependent induction of cell death (Fig. 4A). In a separate set of experiments, we treated U937 cells with 1, 2, or 5 ng/mL RT for 1 h at 37 °C. After this, free RT was removed via centrifugation and washing and the cells were incubated an additional 4 h. Supernatants were used to treat A549 cells for 24 h at 37 °C. A549 cell death induced by 0.5 ng/mL purified RT and 100 ng/mL FasL was not significantly different from death induced by supernatants derived from U937 cells treated with 1 ng/mL RT (Fig. 4A). Therefore, we considered these to be equivalent lytic doses and compared them throughout the remainder of this report. For the following experiments, we treated A549 cells with 0.5 ng/mL purified RT and 100 ng/mL purified FasL or with supernatants derived from U937 cells treated with 1 ng/mL RT. When A549 cells were treated with zVAD-fmk, death by purified RT and FasL was prevented but death by supernatants from U937 cells was not affected (Fig. 4B). The ability of zVAD-fmk to inhibit A549 cell death by purified RT and FasL is consistent with our previous report, even though caspases do not drive this death [21]. The cathepsin inhibitor, CATI-1, prevented A549 cell death by purified RT and FasL (Fig. 4C), consistent with our previous report [21]. CATI-1 had no effect on A549 cell death induced by supernatants from RT-treated U937 cells (Fig. 4C). To further determine

**Fig. 4.** Death of bystander A549 cells differs from A549 cell death induced by purified RT and Fas ligand (FasL). A.) WST-1 assay showing A549 cell death induced by purified RT (0.1, 0.2, and 0.5 ng/mL) and FasL (100 ng/mL) vs. A549 cell death induced by supernatants from U937 cells treated with 1, 2, or 5 ng/mL RT. A549 cell death induced by purified RT (0.5 ng/mL) and FasL (100 ng/mL) was not significantly different from A549 cell death induced by supernatant from U937 cells treated with 1 ng/mL RT. A549 cells were treated with purified RT (0.5 ng/mL) and FasL (100 ng/mL) or supernatants from U937 cells treated with 1 ng/mL RT for 5 h at 37°C. For Figs B-E, A549 cells were incubated with purified RT (0.5 ng/mL) and FasL (100 ng/mL) or supernatants from U937 cells treated with 1 ng/mL RT (RT SUPs) for 24 h at 37°C followed by WST-1 assay. B.) Flowchart describing experimental setup for direct and bystander A549 WST-1 viability assays. C.)



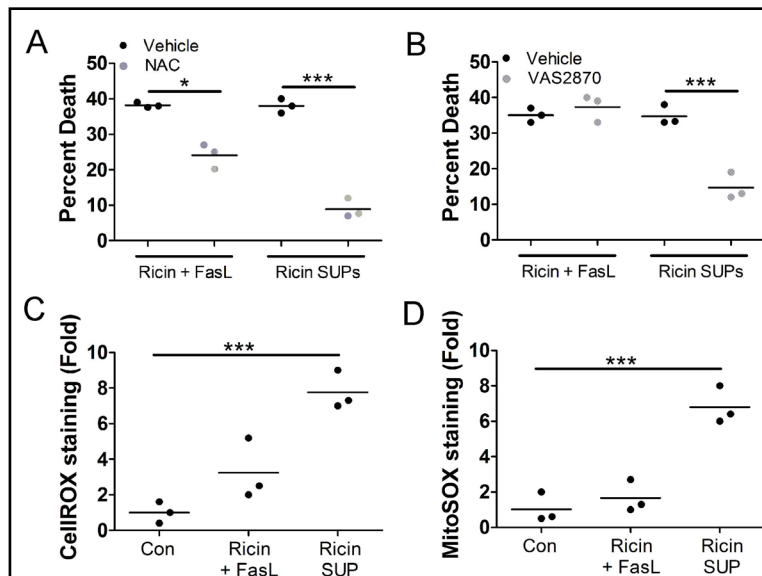
The pan-caspase inhibitor, zVAD-fmk and D.) the cathepsin inhibitor, CATI-1, prevented A549 cell death induced by purified RT and FasL but did not prevent death of bystander A549 cells treated with U937 cell supernatants. A549 cell death induced by purified RT and FasL or U937 cell supernatants was not affected by E.) caspase-1 inhibitor, zVAD-fmk or F.) ferroptosis inhibitor, ferrostatin. Vehicle = DMSO. Results are from 3 independent experiments. Each dot in the graphs represents an independent experiment. Two-way ANOVA with Bonferroni posttest. \*\*\*p<0.001.

the mode of cell death we treated A549 cells with the caspase-1 inhibitor, zYVAD-fmk, which prevents pyroptosis [42], or ferrostatin, an inhibitor of ferroptosis [43]. Neither inhibitor affected A549 cell death induced by purified RT and FasL or A549 cell death induced by supernatants derived from RT-treated U937 cells (Fig. 4D-E). These results clearly indicate that there is a fundamental difference in the mode of cell death induced by purified RT and FasL vs. supernatants derived from RT-treated U937 cells.

*Death of bystander A549 cells depends on reactive oxygen species (ROS), HMGB1, and the receptor for advanced glycation end products (RAGE)*

Next, we determined if reactive oxygen species (ROS) were involved in the death of bystander A549 cells. For this, we treated A549 cells with 0.5 ng/mL purified RT and 100 ng/mL purified FasL or with supernatants derived from U937 cells treated with 1 ng/mL RT in the presence or absence of the antioxidant, N-acetylcysteine (NAC), followed by WST-1 viability assay. Consistent with our previous report, NAC partially inhibited A549 cell death by purified RT and FasL (Fig. 5A). There was an even greater inhibition by NAC, when A549 cell death was induced by RT-treated U937 cell supernatants (Fig. 5A). To determine the contribution from NADPH oxidases (NOX), we ran a similar experiment with the NOX inhibitor, VAS2870 [44], used in place of NAC. While it did not inhibit A549 cell death by purified RT and FasL, it did inhibit cell death by supernatants from RT-treated U937 cells (Fig. 5B). To measure oxidative stress, we treated A549 cells with 0.5 ng/mL purified RT and 100 ng/mL purified FasL or with supernatants derived from U937 cells treated with 1 ng/mL RT followed by staining with cellROX green reagent and flow cytometry. There was an approximately 8-fold increase in cellROX staining in A549 cells treated with supernatants from RT-treated U937 cells, indicating increased oxidative stress (Fig. 5C). To measure mitochondrial ROS, we conducted a similar experiment using mitoSOX red reagent in place of cellROX green. There was an approximately 6-fold increase in mitoSOX staining in A549 cells treated with supernatants from RT-treated U937 cells, indicating increased mitochondrial ROS (Fig. 5D).

**Fig. 5.** Supernatants from U937 cells treated with RT induce reactive oxygen species (ROS) in bystander A549 cells. For A-B, A549 cells were treated with purified RT (0.5 ng/mL) and FasL (100 ng/mL) or supernatants from U937 cells treated with 1 ng/mL RT (RT SUPs) for 5 h at 37°C. A549 cells were treated with purified RT and FasL or U937 cell supernatants for 24 h at 37°C followed by WST-1 assay. A.) The antioxidant, N-acetylcysteine, prevents A549 cell death induced by purified RT and FasL or U937 cell supernatants. B.)



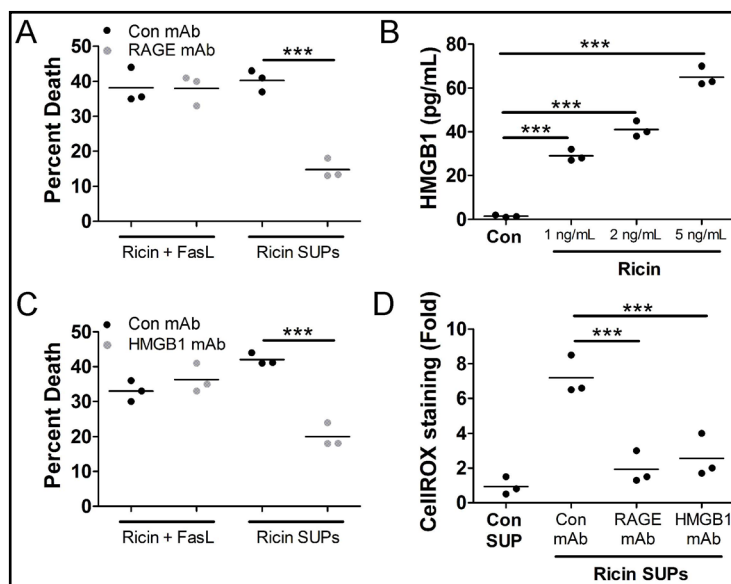
The NADPH oxidase inhibitor, VAS2870, prevents A549 cell death induced by supernatants derived from RT-treated U937 cells. For C-D, A549 cells were treated with purified RT (0.5 ng/mL) and FasL (100 ng/mL) or supernatants from U937 cells treated with 1 ng/mL RT (RT SUPs) for 2 h at 37°C followed by staining for ROS and flow cytometry. C.) CellROX staining increases significantly when A549 cells are treated with supernatants from RT-treated U937 cells indicating increased oxidative stress. D.) MitoSOX staining increases significantly when A549 cells are treated with supernatants from RT-treated U937 cells indicating increased mitochondrial ROS. Con = supernatants from untreated U937 cells. Results are from 3 independent experiments. Each dot in the graphs represents an independent experiment. Two-way ANOVA with Bonferroni posttest. \*p<0.05, \*\*\*p<0.001.

That A549 cell death induced by supernatants derived from RT-treated U937 cells depends heavily on ROS suggests that other factors may be involved in death of bystander A549 cells. The receptor for advanced glycation end products (RAGE) induces ROS upon ligation [45–47], therefore we tested if RAGE was involved in the death of bystander A549 cells. For this, we treated A549 cells with 0.5 ng/mL purified RT and 100 ng/mL purified FasL or with supernatants derived from U937 cells treated with 1 ng/mL RT in the presence or absence of a RAGE neutralizing mAb followed by WST-1 viability assay. Death of bystander A549 cells was greatly inhibited by the RAGE neutralizing mAb (*Fig. 6A*). A common ligand for RAGE is the nuclear protein HMGB1, which is released from necrotic cells [48, 49]. To determine if U937 cells release HMGB1 following RT-induced apoptosis, we treated U937 cells with 1, 2, or 5, ng/mL RT for 1 h. Free RT was then removed by centrifugation and washing and the cells were incubated an additional 4 h. Following this, supernatants were subjected to HMGB1 ELISA. This experiment determined that there is a dose-dependent increase in the release of HMGB1 from U937 cells treated with RT (*Fig. 6B*). To determine if released HMGB1 drives the death of bystander A549 cells, we treated A549 cells with 0.5 ng/mL purified RT and 100 ng/mL purified FasL or with supernatants derived from U937 cells treated with 1 ng/mL RT in the presence or absence of an HMGB1 neutralizing mAb followed by WST-1 viability assay. Indeed, death of bystander A549 cells was prevented when the HMGB1 neutralizing mAb was administered (*Fig. 6C*). Moreover, both the RAGE and HMGB1 neutralizing mAbs prevented the increase in cellROX staining in bystander A549 cells (*Fig. 6D*).

#### Death of bystander A549 cells is driven by necroptosis

The cell death pathway of necroptosis depends on and is driven by ROS [33–35, 50], therefore, we determined if bystander A549 cells die via this pathway. For this, we treated A549 cells with 0.5 ng/mL purified RT and 100 ng/mL purified FasL or with supernatants

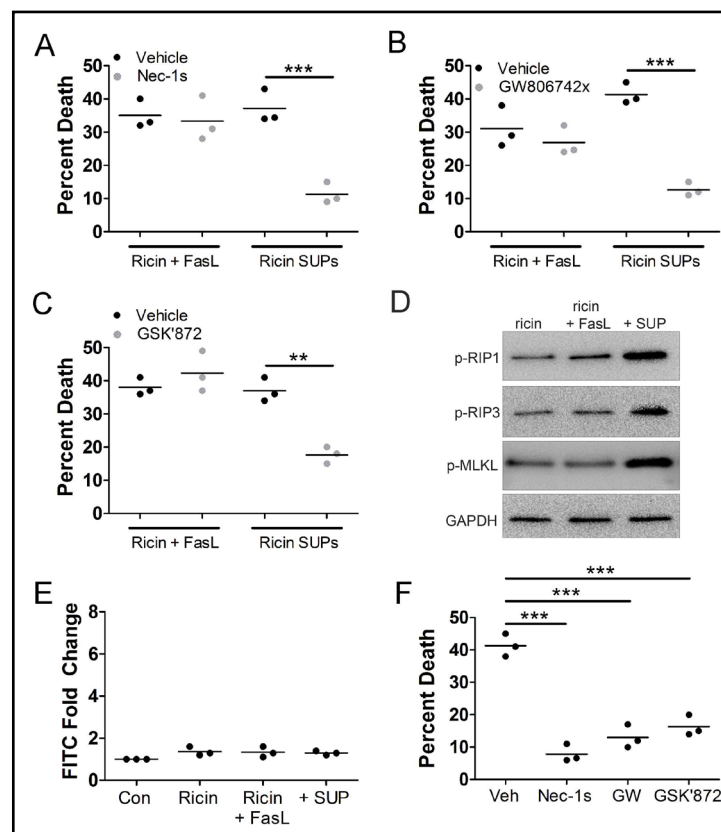
**Fig. 6.** Death of bystander A549 cells depends on HMGB1 and receptor for advanced glycation end products (RAGE). A.) A549 cells were treated with purified RT (0.5 ng/mL) and FasL (100 ng/mL) or supernatants from U937 cells treated with 1 ng/mL RT (RT SUPs) for 5 h at 37°C. A549 cells were treated for 24 h at 37°C followed by WST-1 assay. A549 cell death induced by U937 cell supernatants was prevented when A549 cells were pretreated with neutralizing mAbs against RAGE (1 µg/mL). B.) U937 cells were treated with 1, 2, or 5 ng/mL RT for 5 h at 37°C. Supernatants were removed and subjected to



HMGB1 ELISA. There is a dose dependent increase in the release of HMGB1 from U937 cells following RT treatment. Con SUP = untreated U937 cells. C.) Cells were treated as described in part A except a different neutralizing mAb (1 µg/mL) was used. A549 cell death induced by U937 supernatants was prevented when an HMGB1 neutralizing mAb was added to the supernatant. D.) A549 cells were treated with neutralizing mAbs and supernatants from U937 cells treated with 1 ng/mL RT for 5 h at 37°C followed by cellROX green staining and flow cytometry. The increased staining in cellROX in bystander A549 cells is prevented by neutralizing mAbs against RAGE and HMGB1. Results are from 3 independent experiments. Each dot in the graphs represents an independent experiment. Two-way ANOVA with Bonferroni posttest. \*\*\*p<0.001.

derived from U937 cells treated with 1 ng/mL RT in the presence or absence of necrostatin-1s (nec-1s, RIP1 inhibitor) [38], GW806742x (MLKL inhibitor) [51], or GSK'872 (RIP3 inhibitor) [52] followed by WST-1 viability assay. Death of bystander A549 cells was prevented by all 3 inhibitors (Fig. 7A-C). To confirm the activation of RIP1, RIP3, and MLKL in bystander A549 cells, we treated them with 0.5 ng/mL purified RT and 100 ng/mL purified FasL or with supernatants derived from U937 cells treated with 1 ng/mL RT followed by preparation of lysates and western blot. In A549 cells treated with supernatants derived from U937 cells treated with RT, there was a robust increase in the phosphorylation of RIP1, RIP3, and MLKL (Fig. 7D). These results collectively indicate that bystander A549 cells die by necroptosis. Indeed, when A549 cells were treated with 0.5 ng/mL purified RT, 100 ng/mL FasL, and 100 ng/mL HMGB1 they died in a manner that was prevented by nec-1s, GW806742x, and GSK'872 (Fig. 7E).

**Fig. 7.** A549 cell death induced by supernatants from RT-treated U937 cells is necroptosis. A549 cells were treated with RT (0.5 ng/mL) and FasL (100 ng/mL) or supernatants from U937 cells treated with 1 ng/mL RT (RT SUPs) for 5 h at 37°C. A549 cells were treated for 24 h at 37°C followed by WST-1 assay. A549 cell death induced by U937 cell supernatants was prevented by A.) RIP1 inhibitor, necrostatin-1s (nec-1s), B.) MLKL inhibitor, GW806742x and C.) RIP3 inhibitor, GSK'872. D.) A549 cells were treated with RT (0.5 ng/mL) and FasL (100 ng/mL) or supernatants from U937 cells treated with 1 ng/mL RT (RT SUPs) for 5 h at 37°C. A549 cells were treated for 2 h at 37°C followed by cell lysis, SDS-PAGE, and western blot. The phosphorylated forms of RIP1, RIP3, and MLKL (p-RIP1, p-RIP3, and p-MLKL, respectively) increase in A549 cells after exposure to supernatants from U937 cells treated with RT. E.) A549 cells were treated with RT (0.5 ng/mL) and FasL (100 ng/mL) or supernatants from U937 cells treated with 1 ng/mL RT (RT SUPs) for 5 h at 37°C. A549 cells were treated for 2 h at 37°C followed by FLICA staining for caspase-3/7 activity. There does not appear to be activation of caspases-3 and -7 in any condition. F.) A549 cells were treated with 0.5 ng/mL purified RT, 100 ng/mL FasL, and 100 ng/mL HMGB1 in the presence or absence of necroptosis inhibitors for 24 h at 37°C followed by WST-1 viability assay. Nec-1s, GW806742x (GW), and GSK'872 prevented A549 cell death by purified RT, FasL, and HMGB1. Results are from 3 independent experiments. Each dot in the graphs represents an independent experiment. Two-way ANOVA with Bonferroni posttest. \*\*p<0.01, \*\*\*p<0.001.



## Discussion

In this report, we demonstrate that RT-induced death of U937 cells leads to death of bystander A549 cells. Consistent with numerous previous reports [29, 30, 53], RT induced apoptosis of U937 cells. This apoptosis was critical for the death of bystander A549 cells as the inhibition of U937 cell apoptosis prevented bystander A549 cell death (Fig. 2). The death of bystander A549 cells depended on the release of RT, FasL, and HMGB1 from apoptotic U937 cells. These factors caused an increase in cellular and mitochondrial ROS leading to the death of these bystander A549 cells by necroptosis. This agrees with what we know about the activation of necroptosis as ROS have been shown to be critical for the activation of RIP1 and necroptosis [35]. We propose that this bystander necroptosis may contribute to the severe proinflammatory response observed in the lungs of mice and non-human primates following inhalation of RT.

Previously, we analyzed A549 cell death by purified RT and FasL and determined that it was a form of cathepsin-dependent death [21]. We compared that cell death to the death of bystander A549 cells, which is the focus of this report, as both instances of cell death involved exogenous RT and FasL (Fig. 3) [21]. We determined early in this report that there were fundamental differences in each instance of cell death. The death of bystander A549 cells was not driven by cathepsins nor was it inhibited by zVAD-fmk (Fig. 4), which inhibits A549 cell death by purified RT and FasL [21]. This led to us identifying additional contributing factors to the death of bystander A549 cells. There was a higher degree of dependence on ROS during bystander A549 cell death vs. A549 death by purified RT and FasL (Fig. 5). As a result, we identified that U937 cells treated with RT also release HMGB1 following apoptosis (Fig. 6). This released HMGB1 and its receptor, RAGE, on A549 cells cause the increase in ROS (Fig. 6). It is likely that this robust increase in ROS influences bystander A549 cells to undergo necroptosis (Fig. 7).

We speculate that the release of FasL and HMGB1 from monocytes attacked by RT may increase the toxicity of RT against cells *in vivo*, including lung epithelial cells. This death of bystander lung epithelial cells may reveal new therapeutic targets against RT toxicity. The involvement of extracellular FasL and HMGB1 in the death of bystander A549 cells could mean that they may be viable therapeutic targets for neutralizing mAbs against RT toxicity in addition to RT itself. The dependence of bystander A549 cell death on ROS means that antioxidants as well as inhibitors of NADPH oxidase may serve as viable therapeutic options against RT toxicity. If targeting cell death pathways, specifically, it would be logical to target several different pathways. This is reasonable as RT induces apoptosis of U937 monocytes/macrophages while bystander A549 lung epithelial cells undergo necroptosis (Fig. 1 & 7). *In vivo*, there may be additional exogenous factors as well as cell death pathways which may need to be targeted to limit RT-induced toxicity. This work may have relevancy to cancer targeting as we have conducted this work using cancerous cell lines. The gene for RT could be transfected into tumor cells [54] to eliminate them. The potency of this approach may be improved in combination with FasL and/or HMGB1.

## Acknowledgements

We acknowledge Jennifer Doering and Ying-hui Rong of the Wadsworth Center (NYS Department of Health) for their technical insight.

### Author Contributions

conceptualization, T.J.L and N.J.M.; methodology, T.J.L. and M.A.D.; formal analysis, T.J.L. and M.A.D.; investigation, A.L.H., C.G.K., M.H., M.V. and J.Q.; data curation, T.J.L.; writing—original draft preparation, T.J.L.; writing—review and editing, T.J.L., M.A.D., and N.J.M.; supervision, T.J.L. and M.A.D.; project administration, T.J.L.; funding acquisition, T.J.L. and N.J.M.

### Funding Sources

This research was funded by the National Heart, Lung, and Blood Institute (NHLBI) of the National Institutes of Health (NIH), grant number NIH 2R15-HL135675-02 to T.J.L and the National Institute of Allergy and Infectious Diseases (NIAID) of the NIH, grant number AI125190 to N.J.M.

### Statement of Ethics

The authors have no ethical conflicts to disclose.

### Disclosure Statement

The authors have no conflicts of interest to declare.

### References

- 1 Bradberry SM, Dickers KJ, Rice P, Griffiths GD, Vale JA. Ricin poisoning. *Toxicol Rev* 2003;22:65–70.
- 2 Audi J, Belson M, Patel M, Schier J, Osterloh J. Ricin poisoning a comprehensive review. *J Am Med Assoc* 2005;294:2342–1251.
- 3 Lopez Nunez OF, Pizon AF, Tamama K. Ricin Poisoning after Oral Ingestion of Castor Beans: A Case Report and Review of the Literature and Laboratory Testing. *Journal of Emergency Medicine* 2017;53:e67–71.
- 4 Anderson PD. Bioterrorism: Toxins as weapons. *J Pharm Pract* 2012;25:121–129.
- 5 Gopalakrishnakone P, Balali-Mood M, Llewellyn L, Singh BR. Biological toxins and bioterrorism. 2015 DOI: 10.1007/978-94-007-5869-8
- 6 Falach R, Sapoznikov A, Gal Y, Israeli O, Leitner M, Seliger N, et al. Quantitative profiling of the *in vivo* enzymatic activity of ricin reveals disparate depurination of different pulmonary cell types. *Toxicol Lett* 2016;258:11–19.
- 7 Lord JM, Roberts LM, Robertus JD. Ricin: structure, mode of action, and some current applications. *The FASEB Journal* 2018;8:201–208.
- 8 Taubenschmid J, Stadlmann J, Jost M, Klokk TI, Rillahan CD, Leibbrandt A, et al. A vital sugar code for ricin toxicity. *Cell Res* 2017;27:1351–1364.
- 9 Spooner RA, Michael Lord J. Ricin trafficking in cells. *Toxins (Basel)* 2015;7:49–65.
- 10 Spooner RA, Watson PD, Marden CJ, Smith DC, Moore KAH, Cook JP, et al. Protein disulphide-isomerase reduces ricin to its A and B chains in the endoplasmic reticulum. *Biochemical Journal* 2004;383:285–293.
- 11 Endo Y, Tsurugi K. The RNA N-glycosidase activity of ricin A-chain. *Nucleic Acids Symp Ser* 1988;:139–142.
- 12 Sperti S, Montanaro L, Mattioli A, Stirpe F. Inhibition by ricin of protein synthesis *in vitro* : 60S ribosomal subunit as the target of the toxin ( Short Communication ). *Biochemical Journal* 1973;136:813–815.
- 13 Shi X, Khade PK, Sanbonmatsu KY, Joseph S. Functional role of the sarcin-ricin loop of the 23s rRNA in the elongation cycle of protein synthesis. *J Mol Biol* 2012;419:125–138.
- 14 Griffiths GD, Phillips GJ, Holley J. Inhalation toxicology of ricin preparations: Animal models, prophylactic and therapeutic approaches to protection. *Inhal Toxicol* 2007;19:873–887.
- 15 David J, Wilkinson LJ, Griffiths GD. Inflammatory gene expression in response to sub-lethal ricin exposure in Balb/c mice. *Toxicology* 2009;264:119–130.
- 16 Wilhelmssen CL, Pitt MLM. Lesions of acute inhaled lethal ricin intoxication in rhesus monkeys. *Vet Pathol* 1996;33:296–302.
- 17 Matthay MA, Zemans RL, Zimmerman GA, Arabi YM, Beitler JR, Mercat A, et al. Acute respiratory distress syndrome. *Nat Rev Dis Primers*. 2019 DOI: 10.1038/s41572-019-0069-0
- 18 Pincus SH, Bhaskaran M, Brey RN, Didier PJ, Doyle-Meyers LA, Roy CJ. Clinical and pathological findings associated with aerosol exposure of macaques to ricin toxin. *Toxins (Basel)* 2015;7:2121–2133.
- 19 Gal Y, Mazor O, Falach R, Sapoznikov A, Kronman C, Sabo T. Treatments for pulmonary ricin intoxication: Current aspects and future prospects. *Toxins (Basel)*. 2017;9(10). DOI: 10.3390/toxins9100311

- 20 Rong Y, Westfall J, Ehrbar D, LaRocca T, Mantis NJ. TRAIL (CD253) Sensitizes Human Airway Epithelial Cells to Toxin-Induced Cell Death. *mSphere*. 2018;3(5). DOI: 10.1128/msphere.00399-18
- 21 Hodges, Kempen, McCaig, Parker, Mantis, LaRocca. TNF Family Cytokines Induce Distinct Cell Death Modalities in the A549 Human Lung Epithelial Cell Line when Administered in Combination with Ricin Toxin. *Toxins (Basel)* 2019;11:450.
- 22 Korcheva V, Wong J, Lindauer M, Jacoby DB, Iordanov MS, Magun B. Role of apoptotic signaling pathways in regulation of inflammatory responses to ricin in primary murine macrophages. *Mol Immunol* 2007;44:2761–1771.
- 23 Wong J, Korcheva V, Jacoby DB, Magun B. Intrapulmonary delivery of ricin at high dosage triggers a systemic inflammatory response and glomerular damage. *American Journal of Pathology* 2007;170:1497–510.
- 24 DaSilva L, Cote D, Roy C, Martinez M, Duniho S, Pitt MLM, et al. Pulmonary gene expression profiling of inhaled ricin. *Toxicol* 2003;41:813–822.
- 25 Lindauer M, Wong J, Magun B. Ricin toxin activates the NALP3 inflammasome. *Toxins (Basel)* 2010;2:1500–1514.
- 26 Wong J, Magun BE, Wood LJ. Lung inflammation caused by inhaled toxicants: A review. *International Journal of COPD* 2016;11:1391–1401.
- 27 Sapozhnikov A, Falach R, Mazor O, Alcalay R, Gal Y, Seliger N, et al. Diverse profiles of ricin-cell interactions in the lung following intranasal exposure to ricin. *Toxins (Basel)*. 2015;7:4817–4831.
- 28 Lindauer ML, Wong J, Iwakura Y, Magun BE. Pulmonary Inflammation Triggered by Ricin Toxin Requires Macrophages and IL-1 Signaling. *The Journal of Immunology* 2009;183:1419–1426.
- 29 Tamura T, Sadakata N, Oda T, Muramatsu T. Role of zinc ions in ricin-induced apoptosis in U937 cells. *Toxicol Lett* 2002;132:141–151.
- 30 Hasegawa N, Kimura Y, Oda T, Komatsu N, Muramatsu T. Isolated ricin B-chain-mediated apoptosis in U937 cells. *Biosci Biotechnol Biochem* 2000;64:1422–1429.
- 31 Degterev A, Huang Z, Boyce M, Li Y, Jagtap P, Mizushima N, et al. Chemical inhibitor of nonapoptotic cell death with therapeutic potential for ischemic brain injury. *Nat Chem Biol* 2005;1:112–119.
- 32 Dunai ZA, Imre G, Barna G, Korcsmaros T, Petak I, Bauer PI, et al. Staurosporine induces necroptotic cell death under caspase-compromised conditions in U937 cells. *PLoS One*. 2012;7. DOI: 10.1371/journal.pone.0041945
- 33 LaRocca TJ, Sosunov SA, Shakerley NL, Ten VS, Ratner AJ. Hyperglycemic conditions prime cells for RIP1-dependent necroptosis. *Journal of Biological Chemistry* 2016;291:13753–13761.
- 34 McCaig WD, Patel PS, Sosunov SA, Shakerley NL, Smiraglia TA, Craft MM, et al. Hyperglycemia potentiates a shift from apoptosis to RIP1-dependent necroptosis. *Cell Death Discov* 2018;4:55.
- 35 Deragon MA, McCaig WD, Patel PS, Haluska RJ, Hodges AL, Sosunov SA, et al. Mitochondrial ROS prime the hyperglycemic shift from apoptosis to necroptosis. *Cell Death Discov* 2020;6(1). DOI: 10.1038/s41420-020-00370-3
- 36 Garcia-Calvo M, Peterson EP, Leitig B, Ruel R, Nicholson DW, Thornberry NA. Inhibition of Human Caspases by Peptide-based and Macromolecular Inhibitors\*. 1998. Available from: <http://www.jbc.org>
- 37 Ekert PG, Silke J, Vaux DL. Caspase inhibitors Available from: <http://www.stockton-press.co.uk/cdd>
- 38 Degterev A, Hitomi J, Gemscheid M, Ch'en IL, Korkina O, Teng X, et al. Identification of RIP1 kinase as a specific cellular target of necrostatins. *Nat Chem Biol* 2008;4:313–321.
- 39 Darzynkiewicz Z, Pozarowski P, Lee BW, Johnson GL. Fluorochrome-labeled inhibitors of caspases: Convenient *in vitro* and *in vivo* markers of apoptotic cells for cytometric analysis. *Methods in Molecular Biology* 2011;682:103–114.
- 40 Gerke V, Moss SE. Annexins: From Structure to Function. 2002 DOI: 10.1152/physrev.00030.2001.-Annexins
- 41 Riccardi C, Nicoletti I. Analysis of apoptosis by propidium iodide staining and flow cytometry. *Nat Protoc* 2006;1:1458–1461.
- 42 Miao EA, Rajan J v, Aderem A. Caspase-1-induced pyroptotic cell death. *Immunol Rev* 2011;243:206–214.
- 43 Dixon SJ, Lemberg KM, Lamprecht MR, Skouta R, Zaitsev EM, Gleason CE, et al. Ferroptosis: An iron-dependent form of nonapoptotic cell death. *Cell* 2012;149:1060–1072.

- 44 Wingler K, Altenhoefer SA, Kleikers PWM, Radermacher KA, Kleinschnitz C, Schmidt HHHW. VAS2870 is a pan-NADPH oxidase inhibitor. *Cell Mol Life Sci* 2012;69:3159–3160.
- 45 Basta G, Lazzarini G, del Turco S, Ratto GM, Schmidt AM, de Caterina R. At least 2 distinct pathways generating reactive oxygen species mediate vascular cell adhesion molecule-1 induction by advanced glycation end products. *Arterioscler Thromb Vasc Biol* 2005;25:1401–1407.
- 46 Koulis C, Watson AMD, Gray SP, Jandeleit-Dahm KA. Linking RAGE and Nox in diabetic micro- and macrovascular complications. *Diabetes Metab* 2015;41:272–281.
- 47 Yamagishi S, Maeda S, Matsui T, Ueda S, Fukami K, Okuda S. Role of advanced glycation end products (AGEs) and oxidative stress in vascular complications in diabetes. *Biochim Biophys Acta* 2012;1820:663–671.
- 48 Treutiger CJ, Mullins GE, Johansson A-SM, Rouhiainen A, Rauvala HME, Erlandsson-Harris H, et al. High mobility group 1 B-box mediates activation of human endothelium. *J Intern Med* 2003;254:375–385.
- 49 Schmidt AM, Yan SD, Yan SF, Stern DM. The biology of the receptor for advanced glycation end products and its ligands. *Biochim Biophys Acta* 2000;1498:99–111.
- 50 Vandenabeele P, Galluzzi L, vanden Berghe T, Kroemer G. Molecular mechanisms of necroptosis: an ordered cellular explosion. *Nat Rev Mol Cell Biol* 2010;11:700–714.
- 51 Hildebrand JM, Tanzer MC, Lucet IS, Young SN, Spall SK, Sharma P, et al. Activation of the pseudokinase MLKL unleashes the four-helix bundle domain to induce membrane localization and necroptotic cell death. *Proc Natl Acad Sci U S A* 2014;111:15072–15077.
- 52 Mandal P, Berger SB, Pillay S, Moriwaki K, Huang C, Guo H, et al. RIP3 Induces Apoptosis Independent of Pronecrotic Kinase Activity. *Mol Cell* 2014;56:481–495.
- 53 Oda T, Iwaoka J, Komatsu N, Muramatsu T. Involvement of N-acetylcysteine-sensitive pathways in ricin-induced apoptotic cell death in U937 cells. *Biosci Biotechnol Biochem* 1999;63:341–348.
- 54 Ling C. Cytotoxic genes from traditional Chinese medicine inhibit tumor growth both *in vitro* and *in vivo*. *J Integr Med* 2014;12:483–494.